RESEARCH ARTICLE

Spectral sensitivity of the principal eyes of sunburst diving beetle, *Thermonectus marmoratus* (Coleoptera: Dytiscidae), larvae

Srdjan Maksimovic, John E. Layne and Elke K. Buschbeck*

Department of Biological Sciences, University of Cincinnati, Cincinnati, OH 45221-0006, USA

*Author for correspondence (elke.buschbeck@uc.edu)

SUMMARY

The principal eyes of sunburst diving beetle, *Thermonectus marmoratus*, larvae are among the most unusual eyes in the animal kingdom. They are composed of long tubes connecting bifocal lenses with two retinas: a distal retina situated a few hundred micrometers behind the lens, and a proximal retina that is situated directly beneath. A recent molecular study on first instar larvae suggests that the distal retina expresses a long-wavelength-sensitive opsin (TmLW), whereas the proximal retina predominantly expresses an ultraviolet-sensitive opsin (TmUV II). Using cloning and *in situ* hybridization we here confirm that this opsin distribution is, for the most part, maintained in third instar larvae (with the exception of the TmUV I that is weakly expressed only in proximal retinas of first instar larvae). We furthermore use intracellular electrophysiological recordings and neurobiotin injections to determine the spectral sensitivity of individual photoreceptor cells. We find that photoreceptors of the proximal retina have a sensitivity curve that peaks at 374–375 nm. The shape of the curve is consistent with the predicted absorbance of a single-opsin template. The spectral response of photoreceptors from the distal retina confirms their maximum sensitivity to green light with the dominant λ-peak between 520 and 540 nm, and the secondary β-peak between 340 and 360 nm. These physiological measurements support molecular predictions and represent important steps towards understanding the functional organization of the unusual stemmata of *T. marmoratus* larvae.

Key words: stemmata, opsin, eye, predator.

INTRODUCTION

Animal eyes fall into two broad mechanistic categories: simple lens eyes and compound eyes. The principal eyes of the larvae of the predaceous sunburst diving beetle, *Thermonectus marmoratus* (Coleoptera: Dytiscidae), represent an unusual example of the simple lens type. Unique among known animal eyes, they have truly bifocal lenses (Stowasser et al., 2010). The lenses project light through long tubes to two retinas, which are stacked in series and highly asymmetric: they are horizontally extended and vertically very narrow. The precise function of this unique arrangement is unknown, but somehow it allows these animals to be highly successful visual hunters.

Thermonectus marmoratus has three larval instars, all of which are voracious and highly successful visual predators of soft-bodied prey such as mosquito larvae. They are characterized by six eyes (Fig. 1A) and an eye spot (not illustrated) on each side of the head. Each of the eyes has at least two distinct, tiered regions of photoreceptor cells that constitute a distal and proximal retina (Maksimovic et al., 2009; Mandapaka et al., 2006). Most unusual are the forward-pointing principal eyes, eye 1 (E1) and eye 2 (E2), which share many anatomical characteristics (Fig. 1B). Those include extremely narrow visual fields that extend in the anatomical horizontal plane (illustrated schematically for E1 in Fig. 1C). The larvae perform dorso-ventral head and thorax rotations to visually scan potential prey prior to capture (Buschbeck et al., 2007). In addition, it was recently discovered that the principal eyes possess bifocal lenses (demonstrated for E2) (Stowasser et al., 2010), resulting in two sharp images, each of which could be focused on

its own retina. The degree to which each image is focused depends on chromatic aberration and, ultimately, sensory transduction is influenced by the position and spectral sensitivity of individual receptors. We recently found that in each of the principal eyes of first instar larvae, the distal retina expresses one opsin, predicted to be long-wavelength sensitive (TmLW), whereas the proximal retina expresses two opsins, TmUV I and TmUV II. There, TmUV I is expressed weakly in the dorsal region and TmUV II is expressed strongly throughout the entire proximal retina (Maksimovic et al., 2009). Both of these opsins are predicted by sequence homology to be ultraviolet (UV) sensitive. In the present study we investigated whether the same opsin expression pattern is observed in the penultimate stage, the third instar larvae. In these larger larvae, we were also able to obtain intracellular recordings from photoreceptor cells and thus measure the spectral sensitivity of the two retinas of the dorsally located principal eye (E1).

Most functional investigations of insect eyes have focused on the visual capabilities of the adult compound eyes, though there are a few examples of larval stemmata that rival the sensory capacities of adult compound eyes (Gilbert, 1994). For example, the predatory larvae of the tiger beetle, *Cincindela chinensis*, have sophisticated camera-type eyes (Toh and Mizutani, 1987; Toh and Mizutani, 1994; Toh and Okamura, 2007). Few studies have addressed the spectral sensitivity of larval stemmata, where intracellular measurements of spectral sensitivity are limited to several lepidopteran species (Ichikawa and Tateda, 1980; Ichikawa and Tateda, 1982; Lin et al., 2002). These tend to have green-, blue- and UV-sensitive photoreceptor cells. To our knowledge, there is only one prior
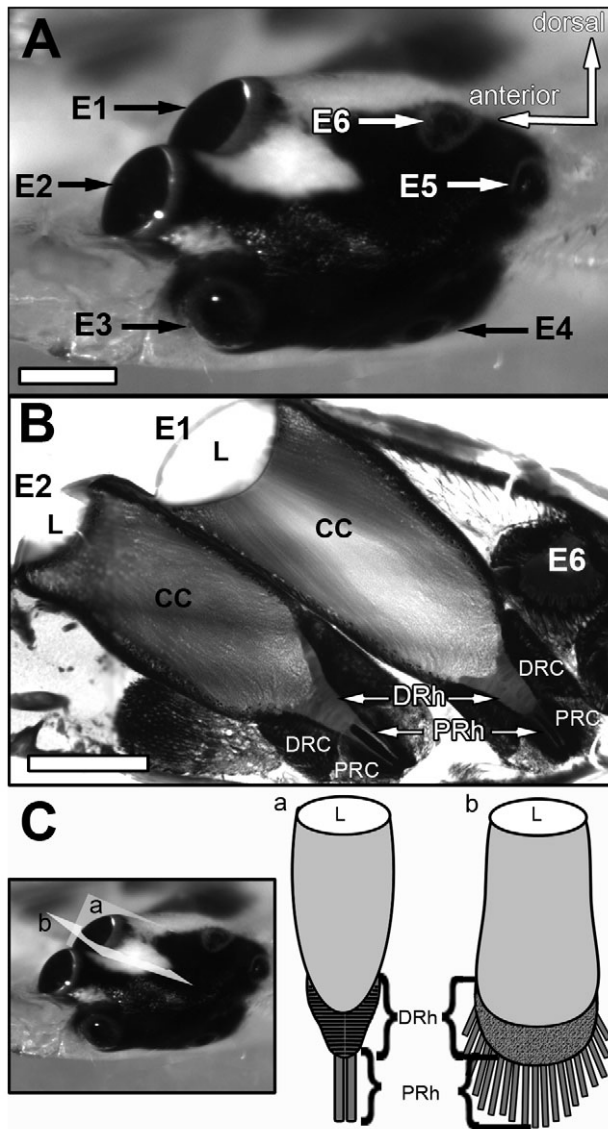
Fig. 1. Principal eyes (E1 and E2) of the third instar larvae of *Thermonectus marmoratus*. (A) Lateral view of the head showing all six eyes (E1–E6). (B) Sagittal section of E1 and E2. Microelectrodes were advanced through E6. (C) Schematic illustration of the anatomical organization of E1, along two axes as indicated in the inset. CC, crystalline-cone-like structure; DRC, distal retina photoreceptor cell bodies; DRh, distal rhabdom; L, lens; PRC, proximal retina photoreceptor cell bodies; PRh, proximal rhabdom. Scale bars, 200 μm.

physiological study within coleopteran larvae, a measurement of the single receptor type of the large stemmata of *C. chinensis* (approximately 525 nm) (Mizutani and Toh, 1995). Considering how few studies exist on stemmatal physiology, the present investigation not only helps us to decipher the unusual organization of the *T. marmoratus* larval principal eyes but also provides insights into visual processing in insect stemmata in general.

MATERIALS AND METHODS
Animals
Adult and larval *T. marmoratus* (Gray 1832) specimens were reared in our laboratory throughout the year. These were offspring of beetles provided by the Insectarium of the Cincinnati Zoo and Botanical Gardens, or from beetles collected between August 2004 and 2008

near Tucson, AZ, USA. Adults were kept in freshwater aquariums at room temperature (RT) and fed daily with freshly killed crickets. After hatching, *T. marmoratus* first instar larvae were separated from adults, moved into a 28°C incubator, and fed with live mosquito larvae and previously frozen blood worms until they developed into the third instars used for these experiments.

Fluorescence *in situ* hybridization
In situ hybridization was performed using RNA probes against opsin mRNA sequences (TmLW, TmUV I and TmUV II) cloned from *T. marmoratus* first instar larvae (Maksimovic et al., 2009). The procedure was identical to the one described, except that in this study we used third instar larvae and focused on the opsin expression patterns in the distal and proximal retina of the principal eyes, E1 and E2.

Electrophysiology
Animal preparation, intracellular recordings and neurobiotin iontophoresis
Animals were first anesthetized by chilling on ice and then immobilized by pouring a warm (~37°C) 2% agarose gel over the entire animal. After hardening, agarose was removed from the front of the head and mandibles were waxed to the bottom of a plastic dish, which subsequently was filled with insect Ringer's solution. Apart from the tip of the abdomen (which is used by the animal for respiration of air) each animal was entirely immersed in insect Ringer's solution. The lens of eye 6 (E6) was removed and a microelectrode was advanced through the underlying tissue, which allowed access to E1 photoreceptors, with minimal injury to the targeted retina. Recordings were performed inside a Faraday cage, on a vibration isolation table (TMC 66-501, Technical Manufacturing Corporation, Peabody, MA, USA). A silver wire that served as the reference electrode was submerged in the insect Ringer's solution. Intracellular recordings and neurobiotin injections were performed with glass microelectrodes (A-M Systems, Inc., Sequim, WA, USA; catalog no. 601000) pulled with a horizontal puller (Sutter Instrument Co. P97, Novato, CA, USA). The microelectrodes were filled with 1% neurobiotin (Vector Laboratories, Inc., Burlingame, CA, USA) in $3 \, mol \, l^{-1}$ KCl, and backed up with $3 \, mol \, l^{-1}$ KCl separated by a small air bubble. Electrode resistances varied from 60 to 130 MΩ when measured in insect Ringer's solution. After positioning the tip of the microelectrode in front of the opening in E6, lights were switched off and the rest of the procedure was performed in the dark. Successful photoreceptor penetration was identified by a drop in membrane potential to –40 to –60 mV, and by the presence of a phasotonic depolarization in response to brief light flashes. After recording, the photoreceptors were injected iontophoretically with neurobiotin by passing a depolarizing current of 2–3 nA for ~15 min. Intracellular recordings and neurobiotin iontophoresis were performed using standard electrophysiological equipment including an A-M Systems Neuroprobe amplifier 1600, a Tektronix oscilloscope 5111A (Tektronix, Inc., Beaverton, OR, USA), an iWorks AD board 118 (iWorks Systems, Inc., Dover, NH, USA) and an A-M Systems audio monitor 3300. Data were stored on a PC using iWorks LabScribe software, and analyzed using a custom-written code in MATLAB (The MathWorks, Inc., Natick, MA, USA).

Monochromatic stimulation
Monochromatic light stimuli were generated using an Oriel Apex 70525 Monochromater Illuminator with a 150 W Xenon arc lamp coupled to an Oriel Cornerstone 130 1/8 m 74000 monochromator (Oriel Instruments, Stratford, CT, USA). The light intensity was

controlled with a Newport circular variable neutral density filter 50G00AV.2 mounted onto a Newport NSR-12 motorized rotator stage with a Newport NewStep Controller NSC200 (Newport Corporation, Irvine, CA, USA) and placed behind the output slit of the monochromator. The duration of the stimulus was controlled with a Uniblitz VCM-D1 shutter (Uniblitz, Rochester, NY, USA), which was placed in front of a UV-VIS optical fiber (model 78278 with 1 mm core diameter; Newport Corporation) that led the light into the Faraday cage. The light was focused on the fiber using a single UV-transmitting converging lens (f=10 cm). The other end of the optical fiber was immersed in insect Ringer's solution and positioned 1–2 mm in front of the lens of E1.

Spectral responses were induced by a modified version of the 'flash method' (Menzel et al., 1986), which employed equiquantal monochromatic light flashes ranging from 300 to 640 nm in 20 nm steps. Prior to the experiment the neutral density filter position was calibrated for each wavelength so that the light intensity emitted by the optical fiber was 6.5×10^{12} photons cm^{-2} s^{-1} (measured with an Ocean Optics USB2000+ spectrometer at the exit of the fiber; Ocean Optics, Inc., Dunedin, FL, USA). After a successful penetration we recorded responses to light from 300 to 640 nm in 20 nm steps, and then in 20 nm steps back to 300 nm. The mean of the two traces was used for analysis. The flashes were 30 ms in duration and had an interval of 10 s. This stimulus duration allowed for a maximum response without saturation, and the interval allowed receptors to fully return to the baseline between stimuli.

After determining the spectral response, we measured the response–stimulus intensity (V–log$I$) function at the peak wavelength. Specifically, we recorded responses elicited by light intensities ranging from $\sim 2 \times 10^{11}$ to $\sim 3.5 \times 10^{14}$ photons cm^{-2} s^{-1} in 0.25 log steps, using filter positions worked out prior to experimentation as above.

Analysis

For the peak wavelength (as determined from the spectral response outlined in the previous section) V–log$I$ responses were recorded and fitted to the hyperbolic Naka–Rushton function, $V/V_{max}=I^n/(I^n+K^n)$ (Menzel et al., 1986; Naka and Rushton, 1966; Skorupski and Chittka, 2010), where V is the response amplitude, V_{max} is the maximum response amplitude, I is the stimulus intensity, K is the stimulus intensity eliciting $V_{max}/2$, and n is the slope of the function. The fitted V–log$I$ function at the peak wavelength was used to estimate V–log$I$ functions for other wavelengths by sliding the fitted curve along the intensity axis to coincide with equiquantal responses measured at each wavelength. Spectral sensitivity was determined as normalized reciprocals of photon numbers needed to elicit equal response amplitudes at all wavelengths. The spectral sensitivity data were fitted to the Govardovskii (Govardovskii et al., 2000) and Stavenga (Stavenga et al., 1993) rhodopsin absorption templates using the MATLAB fminsearch function. These templates generally fit well with invertebrate data, though they are less reliable for wavelengths below ~400 nm (Stavenga, 2010). Photoreceptors of the distal retina could not be recorded for long enough to establish the V–log$I$ function, thus we only report the spectral response trace for these cells.

Histology
Ethyl Gallate staining

Ethyl-Gallate-stained sections were prepared using a standard protocol (Strausfeld and Seyan, 1985) with some minor modifications (Mandapaka et al., 2006). After staining, the *T. marmoratus* heads were dehydrated, embedded in Ultra-Low Viscosity Embedding Medium (Polysciences, Warrington, PA, USA) and serially sectioned at 8 μm.

Neurobiotin tracing

After iontophoresis of neurobiotin, the animals were kept for ~1 h at 4°C to allow for tracer diffusion. The heads were cut off and fixed in 4% paraformaldehyde solution in 0.2 mol l^{-1} Sorensen's buffer (Electron Microscopy Sciences, Hatfield, PA, USA) for 14 to 16 h at 4°C. After washing in Sorensen's buffer for at least 8 h at RT, the tissue was dehydrated through an ethanol series, infiltrated in propylene oxide for ~15 min, and rehydrated. This latter procedure rendered the tissue more porous, allowing for a better penetration of streptavidin. The tissue was then incubated with streptavidin conjugated with Alexa Fluor 568 (Life Technologies Corporation, Carlsbad, CA, USA) diluted 1:200 (working concentration 0.5 μg ml^{-1}) in Sorensen's buffer with 1% Triton X-100 for 14–16 h at RT. After thorough washing with Sorensen's buffer, the decapitated heads were dehydrated in a series of ethanol solutions, embedded in Ultra-Low Viscosity Embedding Medium (Polysciences), serially sectioned at 15 μm, and mounted using Fluoromount-G (SouthernBiotech, Birmingham, AL, USA). Fluorescence images were taken with an Olympus 60806 digital camera (Olympus America Inc., Center Valley, PA, USA) or using the Zeiss LSM 510 laser scanning confocal microscope (Carl Zeiss AG, Oberkochen, Germany), and adjusted for brightness and contrast with Adobe Photoshop CS3 (Adobe Systems Inc., San Jose, CA, USA).

RESULTS

Apart from the relative proportions of some of the tissues (especially the two retinas), the general anatomical organization of the principal eyes in third instars is similar to that of first instars (Mandapaka et al., 2006) (Fig. 1B). In the first part of this study we performed RNA *in situ* hybridization using probes made against three opsin sequences cloned in first instar larvae (TmLw, TmUV I and TmUV II), to determine which opsins are expressed in the distal and proximal retina of the principal eyes of third instar larvae. In the second part we used intracellular recording techniques to directly measure the spectral sensitivity of photoreceptor cells from the distal and proximal retina of E1 in third instar larvae. Because we only managed to record spectral response traces from two photoreceptors from the distal retina of E1, we only report their spectral response data, without performing further spectral or temporal analysis.

Fluorescence *in situ* hybridization

Of the three opsins cloned from *T. marmoratus* first instar larvae, we located expression of two mRNAs, TmLW and TmUV II, in the distal and proximal retinas of the third instar larva principal eyes (Fig. 2). As shown by fluorescence *in situ* hybridization, the cell bodies of the distal retinas (DRC) of both principal eyes express TmLW mRNA (Fig. 3B,C), whereas cell bodies of the proximal retinas (PRC) express TmUV II mRNA (Fig. 3D,E). As expected, the rhabdomeric regions of each retina (DRh and PRh) were not stained well with any of the opsin probes, leaving fairly translucent regions in the centers. We did not find signs of TmUV I mRNA expression in either of the two retinas.

Spectral sensitivities
Proximal retina

As in other invertebrates, such as *Drosophila* (Hardie and Raghu, 2001), the photoreceptors of the proximal retina responded with a graded depolarizing receptor potential to light stimuli with a faster
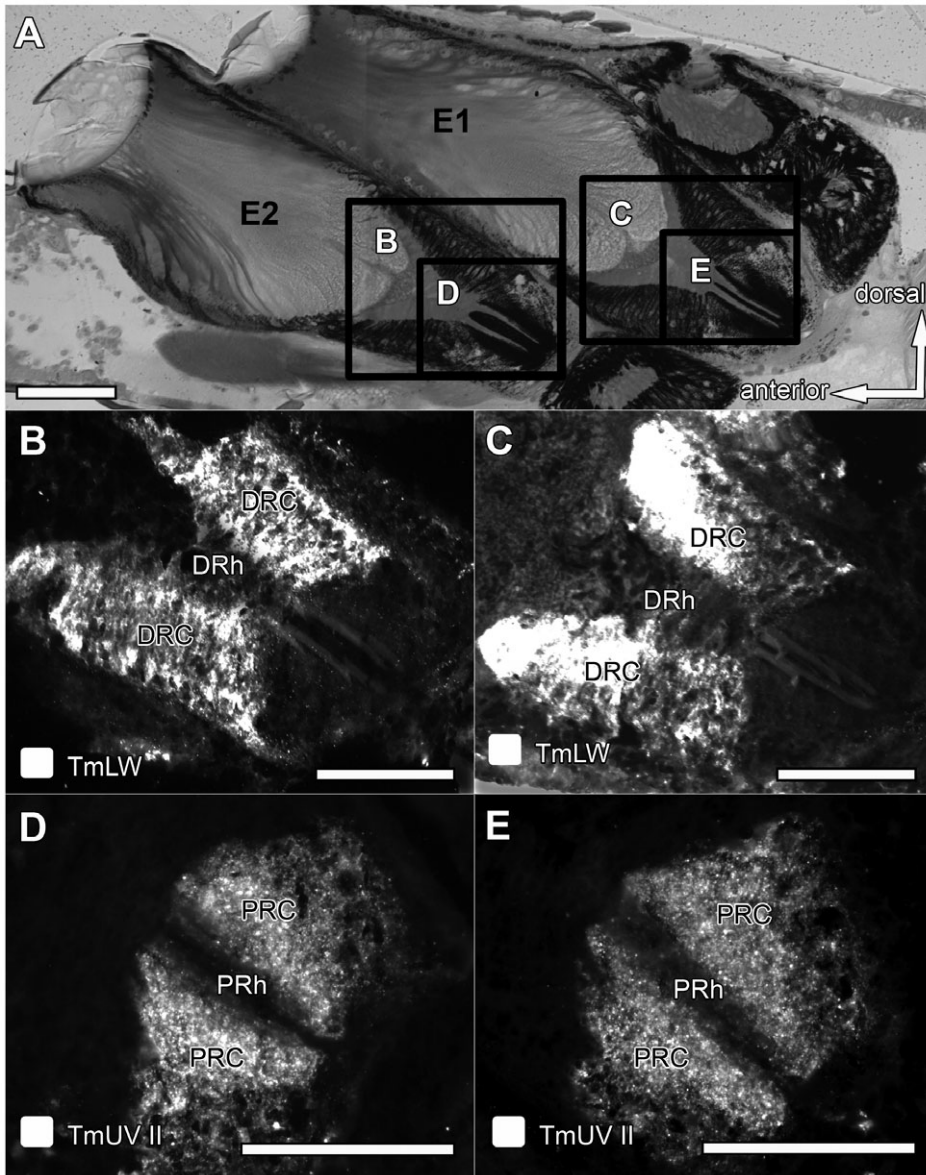
Fig. 2. Distribution of opsin mRNAs in the principal eyes of *T. marmoratus* as examined by *in situ* hybridization. All hybridizations are illustrated in sagittal sections. (A) An overview histological section indicates the positions of images B–E. TmLW mRNA is expressed in the distal retinas of both E1 (C) and E2 (B). TmUV I mRNA is expressed in the proximal retinas of E1 (E) and E2 (D). Scale bars, 100 μm.

rising and a slower falling phase. This can be seen in Fig. 3A, which illustrates normalized flash responses of 20 photoreceptors (one photoreceptor per animal) to a series of different wavelength stimuli. The typical spectral response trace of a single photoreceptor to monochromatic light stimuli (300 to 640 nm) is depicted in Fig. 3B. In this example the photoreceptor cell has a peak response of ~18 mV at 360 nm, which is a typical peak wavelength for the photoreceptors of the proximal retina. Therefore, for the photoreceptors of the proximal retina, the *V*–log*I* function was measured at 360 nm. The *V*–log*I* response and the best fit to the Naka–Rushton function for this unit is shown in Fig. 3C. After measuring the spectral response and the *V*–log*I* function for a total of 12 photoreceptors from the proximal retina, its spectral sensitivity curve was reconstructed (Fig. 4A). The curve has a maximum response at 360 nm with no apparent additional peaks or shoulders, and is well fit by the Govardovskii rhodopsin template (R^2=0.983), which indicates a peak absorbance at λ_{max}=374 nm with a half-width of 75 nm (Fig. 4B). A very similar fit was obtained with the Stavenga template (R^2=0.979), with the peak absorbance at λ_{max}=375 nm with a half-width of 75 nm (Fig. 4B). The templates are slightly narrower than the data, and their fit can be improved by accounting for self-screening (Warrant and Nilsson, 1998), which depends on two parameters: the absorption coefficient of the photoreceptors (*k*) and their length (*l*). A typical value for an invertebrate self-screening absorption coefficient is 0.009 μm^{-1} (Warrant and Nilsson, 1998). In the principal eyes of *T. marmoratus* larvae, rhabdoms of the proximal retina form tightly organized columns (Mandapaka et al., 2006). In third instar larva these are approximately 100 μm long (Fig. 1). Adding these self-screening parameters to the rhodopsin templates (see Warrant and Nilsson, 1998) broadens the absorption curves and improves the fit substantially (Fig. 4C). For the Govardovskii template, the half-width increases from 75 to 88 nm and R^2 from 0.983 to 0.991. The same improvement can be made to the Stavenga template, for which the self-screening correction increases the half-width from 75 to 89 nm and R^2 from 0.979 to 0.985.

Neurobiotin staining revealed that all recorded photoreceptors were part of the proximal retina of E1. Although several of the neurobiotin
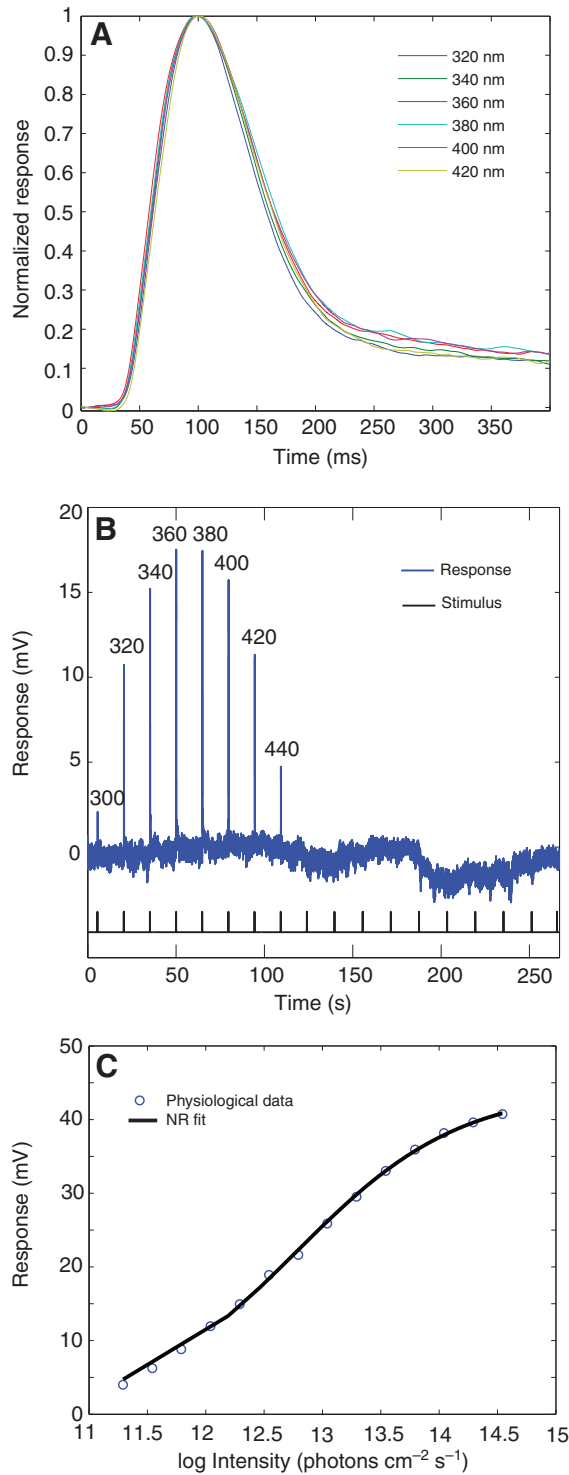
Fig. 3. Physiological characteristics of the proximal photoreceptors of *T. marmoratus*. (A) Mean normalized responses of 20 photoreceptor cells to a series of 30 ms light flashes of different wavelengths (as indicated in the figure). The time point 0 ms coincides with the onset of the 30 ms flash stimulus. (B) The spectral response trace of a single photoreceptor to a series of equiquantal monochromatic flashes (6.5×10^{12} photons cm^{-2} s^{-1}) ranging from 300 to 640 nm (black line) in steps of 20 nm. Spectral stimulation was repeated in the opposite direction (640 to 300 nm) and the mean of the two was taken for further analysis (not illustrated). (C) Response–intensity (*V*–log*I*) function at 360 nm with the best fit of the Naka–Rushton (NR) function. The *V*–log*I* function was recorded over a range from $\sim 2 \times 10^{11}$ to $\sim 3.5 \times 10^{14}$ photons cm^{-2} s^{-1} in 0.25 log steps.
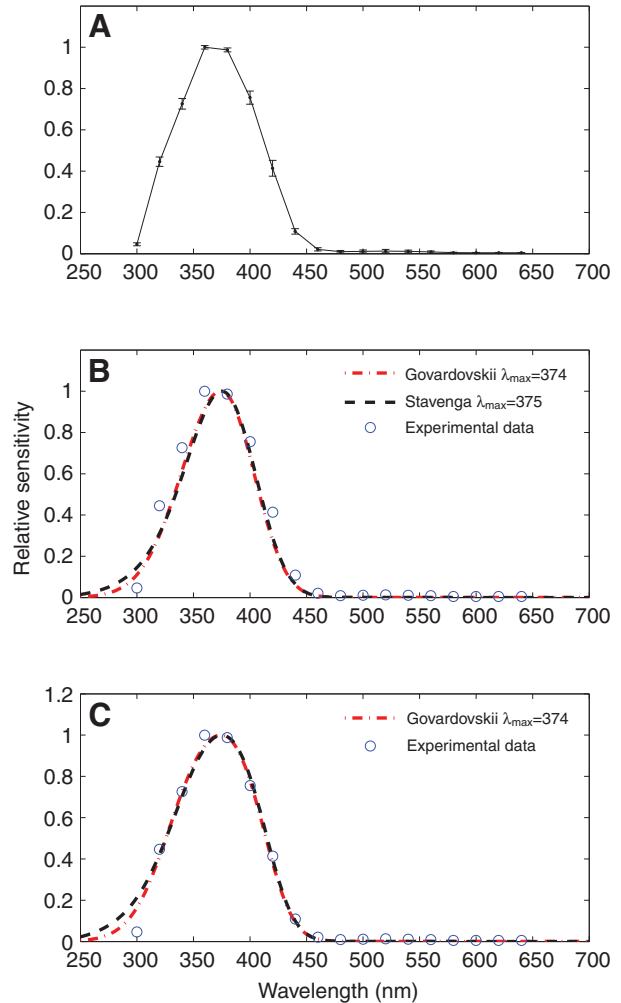

Fig. 4. Spectral sensitivity of *T. marmoratus*. (A) Mean ± s.e.m. normalized spectral sensitivity from 12 units from the proximal retina. For each wavelength, the mean normalized response is indicated by a circle. (B) Both the Govardovskii (red line) and the Stavenga (black line) rhodopsin absorbance models resulted in good fits to our data (circles) with peak absorbance at 374 and 375 nm and correlations of $R^2 = 0.983$ and 0.979, respectively. (C) Including self-screening into the modeling procedure further improves the fit of rhodopsin absorbance templates. Adding $k = 0.009\ \mu m^{-1}$ (dronefly absorption coefficient) and $l = 100\ \mu m$ (photoreceptor length in *T. marmoratus* third instars) broadens the template curve. The half-width increases from approximately 75 nm without self-screening correction to approximately 88 nm with self-screening correction. Correspondingly, there is an increase in the R^2 value from 0.983 to 0.991 for the Govardovski model and from 0.979 to 0.985 for the Stavenga model.

fills stained single cells, some of the preparations labeled two or three closely grouped photoreceptors after a single neurobiotin injection. Fig. 5A shows an example of a single cell filled with neurobiotin in the proximal retina of E1. In contrast, Fig. 5B shows an example in which two photoreceptors were stained, even though neurobiotin iontophoresis was performed only once, after a successful spectral sensitivity measurement from one cell.

Distal retina

Photoreceptors of the distal retina are smaller, and most of our recordings were too brief to successfully characterize their spectral

sensitivity (though many cells were confirmed to respond to green light). We acquired complete spectral response data from two photoreceptors, the mean of which is shown in Fig. 6A. As can be seen from the figure, the peak is in the green (LW) range at 520 nm. The inset shows the peak response of one of those cells to a 520 nm light flash, with an amplitude of only ~5 mV. For the second photoreceptor, the peak response occurred at 540 nm with an amplitude of only ~3.8 mV (data not shown). Weak and noisy responses were a general characteristic of LW photoreceptors. Besides the dominant peak at 520 nm, the cells exhibited a secondary, smaller peak at 360 nm (Fig. 6A). Error bars are relatively large, due to the small sample size. Fig. 6B illustrates fluorescent staining of a LW photoreceptor in the distal retina of E1. We were not able to hold cells long enough to record V-log$I$ curves. However, based on the shape of the spectral response curve, it appears that their peak sensitivity should lie in the 520–540 nm range. A follow-up study with transgenic *Drosophila* currently is underway and will allow us to specify these spectral sensitivity values more precisely.

DISCUSSION

Our findings demonstrate that in third instar larvae, just as in first instar larvae (Maksimovic et al., 2009) UV and LW opsin mRNA expression is clearly separated, closely following morphological distinctions between different retinas. The *in situ* hybridization results suggest that the proximal retina of each eye specifically expresses the TmUV II mRNA, whereas the two distal retinas express the TmLW mRNA (Fig. 2). These results are supported by our electrophysiological data as well. Indeed, photoreceptors in the proximal retina are maximally sensitive in the UV range with λ_{max}=374–375 nm (Fig. 4) and in the distal retina in the green range with a λ_{max} of approximately 520–540 nm (Fig. 6).

UV sensitivity of the proximal retina

In situ hybridization results suggest the presence of a single UV opsin (TmUV II) in the proximal retina of the third instar larvae principal eyes (Fig. 2D,E). Interestingly, in contrast to the first instar larvae principal eyes, in which TmUV I mRNA is weakly expressed in the dorsal half of the proximal retina (Maksimovic et al., 2009), we did not find any TmUV I mRNA expression in the principal eyes of third instars. Therefore, TmUV I is either absent or expressed at levels too low to be detected by our methods. The presence of only one UV opsin in the proximal retina is also supported by our electrophysiological data. The spectral sensitivity curve fits well with templates for single opsins. Specifically, the Govardovskii rhodopsin template (R^2=0.991, N=12) suggests a UV-sensitive opsin with a λ_{max}=374 nm, and the Stavenga template (R^2=0.979) suggests a UV-sensitive opsin with λ_{max}=375 nm.

The rhodopsin templates are based on the absorption of visual pigments only and do not take into account that the photoreceptor responses can be modified by differential light absorption while light passes through various tissues, including the photoreceptors themselves. Thus, they do not take into account the effect of self-screening. As the light travels down the rhabdom of a photoreceptor cell, however, the peak wavelengths are selectively absorbed more than other wavelengths. This filtering results in a slightly higher abundance of relatively less preferred wavelengths as light travels deeper into the rhabdom, effectively broadening the absorption curve (Coates et al., 2006; Warrant and Nilsson, 1998). This likely explains why the spectral sensitivity measurements for the proximal retina are slightly wider than the model spectral sensitivity curve (Fig. 4B). However, including self-screening into the rhodopsin absorbance model broadens the curve and improves the fit (Fig. 4C). Self-
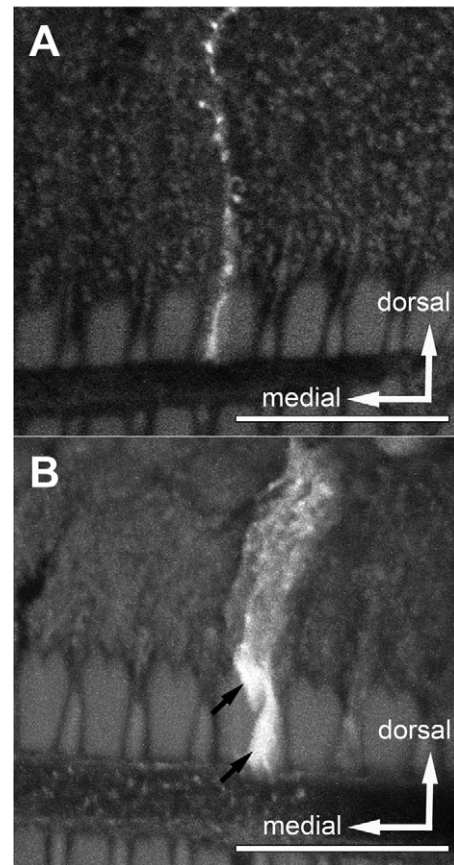

Fig. 5. Photoreceptors of the proximal retina of *T. marmoratus* injected with neurobiotin after successful intracellular measurement. Both images are frontal sections. (A) An example of a single photoreceptor filled with neurobiotin in the proximal retina of E1. (B) An example of two neighboring stained photoreceptors (black arrows) in the proximal retina of E1. In both cases neurobiotin iontophoresis was performed only once, after successfully recording spectral sensitivity measurements from one cell. Scale bars, 20 μm.

screening depends on two parameters: l, the length of the photoreceptor, and k, the absorption coefficient of the photoreceptors. From histology we have estimated l to be approximately 100 μm (see PRh in Fig. 1C). We do not know k for *T. marmoratus* third instars; however, k is known for several other insects (Stavenga, 1976; Warrant and Nilsson, 1998), such as droneflies (k=0.009 μm^{-1}). By using these values to account for self-screening in our models we have substantially improved the goodness of fit. The achieved single opsin correlation is strong – R^2=0.991 for the Govardovskii template and R^2=0.985 for the Stavenga template – confirming that the observed response likely results from a single UV opsin, TmUV II. Although the broadening of the spectral sensitivity curves can result from the presence of multiple opsins with different absorbance maxima (Arikawa et al., 2003), our results do not support this possibility for *T. marmoratus* third instar larvae.

The presence of a single UV opsin in the proximal retina is also consistent with the possibility of polarization sensitivity in this region (Stecher et al., 2010). Polarization sensitivity in insects is most often mediated by UV-sensitive receptor cells (Horvath and Varju, 2004). Moreover, sets of orthogonally oriented photoreceptors in polarization-sensitive eyes should have the same spectral sensitivity to avoid confusion with chromatic stimuli (Wehner and Labhart,

2006). Indeed, Stecher et al. (Stecher et al., 2010) determined that the UV-sensitive proximal retinas of E1 and E2 contain orthogonally oriented neighboring rhabdomeres. Polarization sensitivity could substantially benefit *T. marmoratus* larvae, for example by improving underwater visibility (Marshall and Cronin, 2011).

Some neurobiotin injections led to the labeling of more than one cell (Fig. 5B). It is conceivable that at least some photoreceptors of the proximal retina are coupled through gap junctions, in which case injecting dye into one cell would label the whole group of coupled photoreceptors. However, we do not think that this is the case, because the number of labeled cells per recording greatly varied. The more likely explanation is that additional photoreceptors were stained through leakage of the neurobiotin or during preceding unsuccessful recording attempts.

LW sensitivity of the distal retina

For the photoreceptors of the distal retina, our *in situ* hybridization results from third instar larvae correspond well to those of first instar larvae (Maksimovic et al., 2009), suggesting the presence of only one LW opsin (TmLW). This finding is also supported by our electrophysiological data, which demonstrate the maximal spectral response of distal retina photoreceptors to be in the green range (Fig. 6). Because we were unable to hold photoreceptor cells long enough to record *V*–log*I* functions for these LW-sensitive cells, we did not reconstruct the spectral sensitivity curve for the distal retina. However, the spectral response curve clearly indicates peak sensitivity in the green region, with a dominant peak at 520 nm and a secondary peak at 360 nm. Opsin absorbance at longer wavelengths is characterized with two bands: the main α-band and the low β-band (Govardovskii et al., 2000; Stavenga et al., 1993). Therefore, the two peaks of the spectral response likely represent these two bands. We estimate that λ_{max} is in the green range, approximately 520–540 nm, and that UV sensitivity peaks between 340 and 360 nm. The latter is more variable and thus, harder to estimate, but LW-sensitive opsins typically have β-peaks between 330 and 360 nm (Stavenga et al., 1993), which is in accordance with our results.

Functional implications

Knowledge of the spectral sensitivity of the different photoreceptors substantially advances our ability to understand how the highly unusual larval principal eyes of *T. marmoratus* may function. For example, it has become clear that these spectral sensitivities (given the location of the respective cells) would not allow compensation for lens chromatic aberration, as it has been suggested for the antero-median eyes of jumping spiders (Blest et al., 1981; Land, 1969). Here, photoreceptor tiers closer to the lens are sensitive to the more strongly refracted, shorter wavelengths, whereas deeper photoreceptor layers are excited by the less-refracted, longer wavelengths. Our data suggest the opposite pattern, with a LW-sensitive distal retina and a UV-sensitive proximal retina. Our findings do, however, fit well with the recent discovery that the lenses of *T. marmoratus* are bifocal (demonstrated for E2) (Stowasser et al., 2010), leading to two images, each of which could potentially be focused on its own retina. Given that the distal retina is green sensitive and the proximal retina is UV sensitive, lens chromatic aberration in this case should separate images further, potentially allowing each image to be better resolved independently.

Because of its position and the general eye anatomy (which includes an abundance of screening pigment that shields photoreceptors from off-axis light), the proximal retina can only receive light that passes through the distal retina. Filtering by the
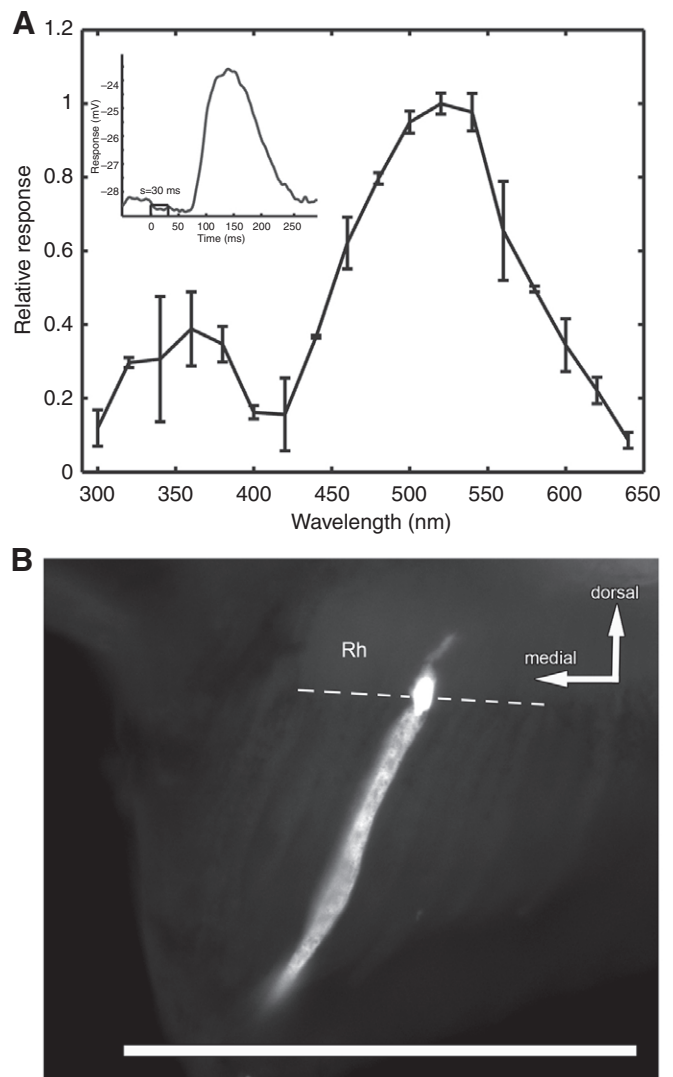

Fig. 6. Photoreceptor sensitivity of the distal retina of *T. marmoratus*. (A) Mean ± s.e.m. normalized spectral response from two photoreceptor cells from the distal retina. The curve has two peaks: the dominant peak shows a maximum response at approximately 520 nm and the smaller peak has a maximum response at approximately 360 nm. The inset shows the waveform of a single impulse response to a 30 ms flash of 520 nm light. (B) Cross-section through the distal retina illustrating a fluorescently labeled cell that was traced back to the distal retina of E1. Dashed line indicates the border between the rhabdomeric regions and the cytoplasm. Scale bar, 100 μm.

distal retina, therefore, could also contribute to the sensitivity curve, perhaps serving as a contrast filter for the proximal retina. LW opsins ($\lambda_{max} \geq 450$ nm) typically have a β-band that absorbs in UV (Stavenga et al., 1993). Therefore, the LW-sensitive distal retina potentially could sharpen the absorbance spectrum of the UV-sensitive proximal retina and increase its imaging contrast. However, our data suggest that significant sharpening of the UV peak is unlikely. If the β-absorbance band of the distal retina had a substantial effect on the proximal retina, then the spectral sensitivity of the proximal retina should deviate from theoretical predictions of single-opsin templates. This is not the case. Instead, the spectral sensitivity curve fits well the opsin templates with $\lambda_{max}=374$ nm (Govardovskii) and $\lambda_{max}=375$ nm (Stavenga). Our results, therefore, suggest that two

features are sufficient to explain the spectral sensitivity curve of the proximal retina: (1) absorbance of a single UV opsin and (2) the self-screening effect. Because the correlation between our experimental data and the template curves is very strong, the contribution of the β-LW band to the sensitivity curve is likely to be relatively minor. Our measurements also demonstrate that the peak absorbency of the *T. marmoratus* opsin compares well with other insect UV photoreceptors, which typically have peak sensitivities at approximately 360 nm (Briscoe, 2008; Stavenga and Arikawa, 2006; Tovee, 1995). A particularly close spectral similarity is observed to the *Drosophila melanogaster* Rh4 opsin, which absorbs maximally at 375 nm (Feiler et al., 1992). Our data also show a spectral response maximum of the green opsin (~520 nm) that is comparable to what has been previously measured for tiger beetle stemmata (525 nm) (Mizutani and Toh, 1995). Based on molecular data, we know that green and UV opsins are present in the adults of the flower beetle *Tribolium* (Jackowska et al., 2007). These beetles also lack a blue opsin, which has been attributed to a loss of this receptor type. Thus far it remains unclear whether a blue opsin is present in adults of *T. marmoratus*. Although the record of spectral sensitivity data among the very large group of Coleoptera is still spotty, considerable variability has been reported (Briscoe and Chittka, 2001). Based on electroretinograms, some other beetles such as *Coccinella* (Polyphaga) lack a spectral sensitivity peak in the blue region, whereas for others such as *Carabus* (Adephaga) and *Photuris* (Polyphaga), specific blue sensitivity has been reported.

It appears that the success of this predator relates to its complex eye organization, in which different retinas are organized differently and may facilitate specific tasks. Task specificity is not unusual in visual systems, and has been found in animals with multiple eyes, such as jellyfish and spiders, where different eyes serve different purposes (Land and Nilsson, 2002; Nilsson et al., 2005). But task specialization can also be present within a single eye, such as the specialized dorsal rim area for polarized light detection in many insects (Labhart and Meyer, 1999). Although it is still unclear how each retina functions, our data support task specialization of the two retinas in two ways: (1) each retina clearly has its own spectral sensitivity, and (2) it appears that proximal photoreceptor cells are more sensitive to light than distal photoreceptor cells. The latter corresponds well to our expectations from the anatomy of these cells (Stecher et al., 2010). The rhabdoms of distal photoreceptor cells are oriented perpendicular to the axis of incoming light, and their relatively small rhabdomeres likely can only absorb a small fraction of the transmitted light. Additional optical, physiological and behavioral experiments will be necessary to establish the true function of these highly unusually organized eyes.

REFERENCES

Arikawa, K., Mizuno, S., Kinoshita, M. and Stavenga, D. G. (2003). Coexpression of two visual pigments in a photoreceptor causes an abnormally broad spectral sensitivity in the eye of the butterfly *Papilio xuthus*. *J. Neurosci.* **23**, 4527-4532.

Blest, A. D., Hardie, R. C., McIntyre, P. and Williams, D. S. (1981). The spectral sensitivities of identified receptors and the function of retinal tiering in the principal eyes of a jumping spider. *J Comp. Physiol. A* **145**, 227-239.

Briscoe, A. D. (2008). Reconstructing the ancestral butterfly eye: focus on the opsins. *J. Exp. Biol.* **211**, 1805-1813.

Briscoe, A. D. and Chittka, L. (2001). The evolution of color vision in insects. *Annu. Rev. Entomol.* **46**, 471-510.

Buschbeck, E., Sbita, S. and Morgan, R. (2007). Scanning behavior by larvae of the predacious diving beetle, *Thermonectus marmoratus* (Coleoptera: Dytiscidae) enlarges visual field prior to prey capture. *J. Comp. Physiol. A* **193**, 973-982.

Coates, M. M., Garm, A., Theobald, J. C., Thompson, S. H. and Nilsson, D.-E. (2006). The spectral sensitivity of the lens eyes of a box jellyfish, *Tripedalia cystophora* (Conant). *J. Exp. Biol.* **209**, 3758-3765.

Feiler, R., Bjornson, R., Kirschfeld, K., Mismer, D., Rubin, G. M., Smith, D. P., Socolich, M. and Zuker, C. S. (1992). Ectopic expression of ultraviolet-rhodopsins in the blue photoreceptor cells of *Drosophila*: visual physiology and photochemistry of transgenic animals. *J. Neurosci.* **12**, 3862-3868.

Gilbert, C. (1994). Form and function of stemmata in larvae of holometabolous insects. *Annu. Rev. Entomol.* **39**, 323-349.

Govardovskii, V. I., Fyhrquist, N., Reuter, T., Kuzmin, D. G. and Donner, K. (2000). In search of the visual pigment template. *Vis. Neurosci.* **17**, 509-528.

Hardie, R. C. and Raghu, P. (2001). Visual transduction in *Drosophila*. *Nature* **413**, 186-193.

Horvath, G. and Varju, D. (2004). *Polarized Light in Animal Vision: Polarization Patterns in Nature*. New York: Springer-Verlag.

Ichikawa, T. and Tateda, H. (1980). Cellular patterns and spectral sensitivitiy of larval ocelli in the swallowtail butterfly *Papilio*. *J. Comp. Physiol. A* **139**, 41-47.

Ichikawa, T. and Tateda, H. (1982). Distribution of color receptors in the larval eyes of four species of Lepidoptera. *J. Comp. Physiol. A* **149**, 317-324.

Jackowska, M., Bao, R., Liu, Z., McDonald, E., Cook, T. and Friedrich, M. (2007). Genomic and gene regulatory signatures of cryptozoic adaptation: loss of blue sensitive photoreceptors through expansion of long wavelength-opsin expression in the red flour beetle *Tribolium castaneum*. *Front. Zool.* **4**, 24.

Labhart, T. and Meyer, E. P. (1999). Detectors for polarized skylight in insects: a survey of ommatidial specializations in the dorsal rim area of the compound eye. *Microsc. Res. Tech.* **47**, 368-379.

Land, M. F. (1969). Structure of the retinae of the principal eyes of jumping spiders (Salticidae: Dendryphantinae) in relation to visual optics. *J. Exp. Biol.* **51**, 443-470.

Land, M. F. and Nilsson, D.-E. (2002). *Animal Eyes*. New York: Oxford University Press.

Lin, J. T., Hwang, P. C. and Tung, L. C. (2002). Visual organization and spectral sensitivity of larval eyes in the moth *Trabala vishnou* Lefebur (Lepidoptera: Lasiocampidae). *Zool. Stud.* **41**, 366-375.

Maksimovic, S., Cook, T. A. and Buschbeck, E. K. (2009). Spatial distribution of opsin-encoding mRNAs in the tiered larval retinas of the sunburst diving beetle *Thermonectus marmoratus* (Coleoptera: Dytiscidae). *J. Exp. Biol.* **212**, 3781-3794.

Mandapaka, K., Buschbeck, E. and Morgan, R. (2006). Twenty-eight retinas but only twelve eyes: an anatomical analysis of the larval visual system of the diving beetle *Thermonectus marmoratus* (Coleoptera: Dytiscidae). *J. Comp. Neurol.* **497**, 166-181.

Marshall, J. and Cronin, T. W. (2011). Polarisation vision. *Curr. Biol.* **21**, R101-R105.

Menzel, R., Ventura, D. F., Hertel, H., Desouza, J. M. and Greggers, U. (1986). Spectral sensitivity of photoreceptors in insect compound eyes. Comparison of species and methods. *J. Comp. Physiol. A* **158**, 165-177.

Mizutani, A. and Toh, Y. (1995). Optical and physiological properties of the larval visual system of the tiger beetle, *Cicindela chinensis*. *J. Comp. Physiol. A* **177**, 591-599.

Naka, K. I. and Rushton, W. A. H. (1966). An attempt to analyse colour reception by electrophysiology. *J. Physiol.* **185**, 556-586.

Nilsson, D.-E., Gislen, L., Coates, M. M., Skogh, C. and Garm, A. (2005). Advanced optics in a jellyfish eye. *Nature* **435**, 201-205.

Skorupski, P. and Chittka, L. (2010). Photoreceptor spectral sensitivity in the bumblebee, *Bombus impatiens* (Hymenoptera: Apidae). *PLoS ONE* **5**, e12049, 1-5.

Stavenga, D. G. (1976). Fly visual pigments. Difference in visual pigments of blowfly and dronefly peripheral retinula cells. *J. Comp. Physiol.* **111**, 137-152.

Stavenga, D. G. (2010). On visual pigment templates and the spectral shape of invertebrate rhodopsins and metarhodopsins. *J. Comp. Physiol. Neural Behav. Physiol.* **196**, 869-878.

Stavenga, D. G. and Arikawa, K. (2006). Evolution of color and vision of butterflies. *Arthropod Struct. Dev.* **35**, 307-318.

Stavenga, D. G., Smits, R. P. and Hoenders, B. J. (1993). Simple exponential functions describing the absorbance bands of visual pigment spectra. *Vision Res.* **33**, 1011-1017.

Stecher, N., Morgan, R. and Buschbeck, E. (2010). Retinal ultrastructure may mediate polarization sensitivity in larvae of the sunburst diving beetle, *Thermonectus marmoratus* (Coleoptera: Dytiscidae). *Zoomorphology* **129**, 141-152.

Stowasser, A., Rapaport, A., Layne, J. E., Morgan, R. C. and Buschbeck, E. K. (2010). Biological bifocal lenses with image separation. *Curr. Biol.* **20**, 1482-1486.

Strausfeld, N. J. and Seyan, H. S. (1985). Convergence of visual, haltere and prosternal inputs at neck motor neurons of *Calliphora erythrocephala*. *Cell Tissue Res.* **240**, 601-615.

Toh, Y. and Mizutani, A. (1987). Visual system of the tiger beetle (*Cicindela chinensis*) larvae. I. Structure. *Zool. Sci.* **4**, 974.

Toh, Y. and Mizutani, A. (1994). Structure of the visual system of the larva of the tiger beetle (*Cicindela chinensis*). *Cell Tissue Res.* **278**, 125-134.

Toh, Y. and Okamura, J. Y. (2007). Morphological and optical properties of the corneal lens and retinal structure in the posterior large sternma of the tiger beetle larva. *Vision Res.* **47**, 1756-1768.

Tovee, M. J. (1995). Ultra-violet photoreceptors in the animal kingdom. Their distribution and function. *Trends Ecol. Evol.* **10**, 455-460.

Warrant, E. J. and Nilsson, D. E. (1998). Absorption of white light in photoreceptors. *Vision Res.* **38**, 195-207.

Wehner, R. and Labhart, T. (2006). Polarization vision. In *Invertebrate Vision* (ed. E. J. Warrant and D.-E. Nilsson), pp. 291-348. Cambridge: Cambridge University Press.